Analysis and validation of a run-of-mine ore grinding mill circuit model for process control

J.D. le Roux[a,*], I.K. Craig[a], D.G. Hulbert[b], A.L. Hinde[c]

[a] *Department of Electrical, Electronic, and Computer Engineering, University of Pretoria, Pretoria, South Africa.*
[b] *Hydrometallurgy Division, Mintek, Randburg, South Africa.*
[c] *AH Consulting, Randburg, South Africa.*

Abstract

A simple and novel non-linear model of a run-of-mine ore grinding mill circuit, developed for process control and estimation purposes, is validated. The model makes use of the minimum number of states and parameters necessary to produce responses that are qualitatively accurate. It consists of separate feeder, mill, sump and hydrocyclone modules that can be connected to model different circuit configurations. The model uses five states: rocks, solids, fines, water and steel balls. Rocks are defined as too large to be discharged from the mill, whereas solids, defined as particles small enough to leave the mill, consist of out-of-specification coarse ore and in-specification fine ore fractions. The model incorporates a unique prediction of the rheology of the slurry within the mill. A new hydrocyclone model is also presented.

The model parameters are fitted to an existing plant's sampling campaign data and a step-wise procedure is given to fit the model to steady-state data. Simulation test results of the model are compared to sampling campaign data of the same plant at different steady-state conditions. The model shows promise in estimating important process variables such as mill power and product particle size and is deemed suitable for process control studies.

Keywords: comminution, grinding, modelling, SAG milling, simulation

1. Introduction

The modelling and simulation of semi-autogenous grinding mills is an indispensable step in the design of a circuit for specific applications (Morrell, 2004; Amestica et al., 1996). The simulation environment can simulate entire comminution circuits and evaluate the designs according to a variety of criteria, e.g. throughput, power draw and product size (Morrell, 2004). The success of the simulation is dependent on the type and accuracy of the models used. A dynamic model needs to be at least qualitatively accurate (i.e. the rate and direction of changes in input, output an internal variables are accurate) if the model is used for the design of control systems or estimating mill variables. A model that is also quantitatively accurate provides a simpler transition between results from simulation to the actual plant (Amestica et al., 1996).

There are two general approaches to model comminution devices besides empirical models that are often used in process control, e.g. (Hulbert et al., 1990; Craig and MacLeod, 1996). A comminution device can be seen as a transform between the feed and a product size distribution where the aim is to represent the phenomenon of breakage rather than the underlying physical process. On the other hand, a model can be based on the interactions of ore particles and elements within the machine on the basis of Newtonian mechanics (Napier-Munn et al., 1999).

The frequency of breakage events is related to the total mass of grinding media and the rate at which the mill rotates. The energy associated with particle breakage is related to the mass of the target rocks and the energy of the grinding media. The minimum required knowledge for a model of a milling circuit is the (Morrell, 2004):

- frequency of breakage events for each size fraction;
- energy associated with each breakage event;
- size distribution of products from each breakage event; and
- transport of slurry through end discharge grates.

The processes above are related to the size reduction, throughput and power response of the mill, which can be predicted simultaneously from one overall model if the model is configured correctly (Morrell, 2004).

Detailed models are popular among researchers and they are often thought to be best or necessary to represent the state of the art. However, they have two potentially serious weaknesses. Firstly, large parameter sets cannot be reasonably fitted accurately from accessible real plant data.

*Corresponding author. Address: Department of Electrical, Electronic, and Computer Engineering, University of Pretoria, Pretoria, South Africa.
Tel.: +27 12 420 2201; Fax: +27 12 362 5000.
Email address: derik.leroux@up.ac.za (J.D. le Roux)

Heavy emphasis is placed on non-linear regression techniques and back-calculation to determine the parameters, in which case small measurement errors can lead to large variances in parameter values (Hinde and Kalala, 2009). Secondly, the detailed models can have internal approximations that transmit and amplify inaccuracies in an unknown way. Generally, detailed models are not invertible in such a way that their parameters and confidence limits can be calculated from data. Because there are so many parameters, a good fit can be obtained by fixing certain parts of the model through wrong adjustments elsewhere.

A unique and novel grinding mill circuit model is considered in this study. The model uses the minimum number of states and parameters necessary for control and estimation purposes. The aim of the model is to provide a simple and theoretically sound model that can be easily implemented and maintained in an advanced process control system without having to resort to purely empirical models. There are potential economic benefits for the operation of grinding mill circuits if such a model is used (Bauer and Craig, 2008; Wei and Craig, 2009a).

Although the model described here has already been presented in Hulbert (2005) and Coetzee et al. (2010), both cases lacked a thorough description and validation of the model. The aim of this article is to present the underlying assumptions and basis of the model, describe how the model works and provide a step-wise procedure to fit the model to plant data. In the article the model is fitted to data from an actual full-scale plant and evaluated as to how well it reconciles with the sampling campaign plant data at various operating conditions. The model will be referred to as the *Hulbert*-model throughout the rest of the article.

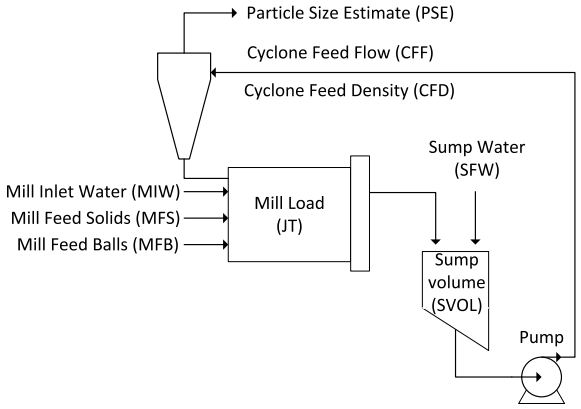

Figure 1: A single-stage closed circuit grinding mill

Table 1: Description of circuit variables

Variable	Description
	Manipulated Variables
MIW	flow-rate of water to the mill [m^3/h]
MFS	feed-rate of ore to the mill [t/h]
MFB	feed-rate of steel balls to the mill [t/h]
SFW	flow-rate of water to the sump [m^3/h]
CFF	flow-rate of slurry to the cyclone [m^3/h]
	Controlled Variables
PSE	product particle size [%]
$LOAD$	volume of charge within the mill [m^3]
$SVOL$	volume of slurry in sump [m^3]
CFD	cyclone feed density [t/m^3]

2. Run-of-Mine Ore Milling Circuit Description

Two types of mills commonly found in the minerals processing industry are ball and semi-autogenous (SAG) mills, which use both ore and steel balls as grinding media (Wei and Craig, 2009b). In the case of a ball mill the ore is crushed before it enters the mill, whereas a SAG mill receives run-of-mine (ROM) ore directly (Stanley, 1987). A SAG mill in a single-stage closed circuit configuration, as shown in Fig. 1, is considered for this study. A description of the variables in Fig. 1, as well as their respective units, can be found in Table 1. These variables are commonly controlled and manipulated in grinding mill circuits (Wei and Craig, 2009b).

The three main elements in Fig. 1 are the mill, the sump and the hydrocyclone. The mill receives four streams: mined ore (MFS), water (MIW), additional steel balls (MFB) to assist with the breakage of ore and underflow from the hydrocyclone. The ground ore in the mill mixes with the water to create a slurry. The volume of charge in the mill is represented by $LOAD$. The slurry in the mill is then discharged to the sump. The slurry from the mill can be discharged either by overflow or through a discharge screen. In the case of the screen, the particle size of the discharged slurry from the mill is limited by the aperture size of the screen. The volume of slurry in the sump is represented by $SVOL$. The slurry in the sump is diluted with water (SFW) before it is passed to the cyclone for classification via a pump. The outflow from the pump is the cyclone feed flow-rate CFF and the density of the cyclone feed is given by CFD. The hydrocyclone is responsible for the separation of the in-specification material and out-of-specification material that is discharged from the sump. The lighter, smaller and in-specification particles in the slurry pass to the overflow of the hydrocyclone, while the heavier, larger and out-of-specification particles pass to the underflow. It is this underflow that is passed to the mill for further grinding. The overflow contains the final product (PSE) that is passed to a downstream process (Stanley, 1987; Wei and Craig, 2009b; Coetzee et al., 2010).

3. The *Hulbert*-model

The circuit shown in Fig. 1 can be described by the reduced complexity non-linear model found in Hulbert (2005) and Coetzee et al. (2010). The approach in the derivation of this model was to use as few fitted parameters as possible while still making the model produce responses that are reasonably accurate and in the right direction. By minimising the number of parameters to fit, redundancy and unmeasurable or uncontrollable degrees of freedom are reduced. This tends to maximise the invertability of the model to obtain parameters from data.

Another aim was to make the model applicable over a wide range of operating regions. To do this, functional forms were made consistent with known physical requirements (e.g. mass conservation) and valid at extreme conditions (e.g. minimum water content in slurry). For example, the Plitt cyclone model can predict underflows with negative water concentrations. The functional form of the Plitt model does not include the useful information that it is impossible for any cyclone to squeeze water out of slurry below some volumetric percentage of water (Nageswararao et al., 2004). Phenomenological modelling is used to provide functional forms where appropriate, but not if it entails the use of more fitted parameters than are absolutely essential to produce the required characteristics.

The model consists of four modules: a feeder, a SAG mill with an end-discharge screen, a sump and a hydrocyclone classifier. All the modules, except for the feeder, can be seen in Fig. 1. The feeder is responsible for the feed of ROM ore, water, balls and the hydrocyclone underflow slurry to the mill. The function of the other three modules - the mill, the sump and hydrocyclone is described briefly in Section 2.

The model uses five states to represent the constituents of charge in the milling circuit. The states are rocks, solids, fines, balls and water. Rocks are ore too large to be discharged from the mill, whereas solids are ore that can be discharged from the mill. The solids consist of the sum of fine and coarse ore, where fine ore is smaller than the product specification size and coarse ore is larger than the product specification size. It is assumed that fines are essentially inseparable from the water found throughout the grinding mill circuit. Balls and rocks are only found in the mill, as they are too large to pass through the apertures in the end-discharge screen. The mill in the circuit is treated as a fully mixed reactor. The manipulated and controlled variables for the model can be seen in Table 1 and Fig. 1.

Each of the four modules and their mathematical descriptions are shown below. For the equations, V denotes a flow-rate in m^3/h and X denotes the states of the model as volumes in m^3. Table 2 provides a description of the subscripts for V and X. The first subscript indicates the module considered, the second subscript specifies which of the five states are considered and in the case of flow-rates the final subscript shows if it is an inflow, outflow or underflow. The nomenclature for the model is shown in Table 3.

Table 2: Description of subscripts for the *Hulbert*-model

Subscript	Description
$X_{\Delta-}$	f-feeder; m-mill; s-sump; c-cyclone
$X_{-\Delta}$	w-water; s-solids; c-coarse; f-fines; r-rocks; b-balls; t-total
$V_{--\Delta}$	i-inflow; o-outflow; u-underflow

Table 3: Feeder, mill and cyclone parameters for the *Hulbert*-model

Parameter	Description
	Feeder and Mill Parameters
α_f	Fraction fines in the ore
α_r	Fraction rock in the ore
α_P	Fractional power reduction per fractional reduction from maximum mill speed
α_{ϕ_f}	Fractional change in kW/fines produced per change in fractional filling of mill
α_{speed}	Fraction of critical mill speed
δ_{P_s}	Power-change parameter for fraction solids in the mill
δ_{P_v}	Power-change parameter for volume of mill filled
D_B	Density of steel balls [t/m^3]
D_S	Density of feed ore [t/m^3]
ε_{sv}	Maximum fraction of solids by volume of slurry at zero slurry flow
ϕ_b	Steel abrasion factor [kWh/t]
ϕ_f	Power needed per tonne of fines produced [kWh/t]
ϕ_r	Rock abrasion factor [kWh/t]
$\varphi_{P_{max}}$	Rheology factor for maximum mill power draw
P_{max}	Maximum mill motor power draw [kW]
v_{mill}	Mill volume [m^3]
$v_{P_{max}}$	Fraction of mill volume filled for maximum power draw
V_V	Volumetric flow per "flowing volume" driving force [h^{-1}]
χ_P	Cross-term for maximum power draw
	Cyclone Parameters
α_{su}	Parameter related to fraction solids in underflow
C_1	Constant
C_2	Constant
C_3	Constant
C_4	Constant
ε_c	Parameter related to coarse split [m^3/h]

3.1. Feeder module

The feeder module divides the ore fed to the mill into various streams. Each stream represents the flow-rate of

one of the five states out of the feeder module into the mill module: water (V_{fwo}), solids (V_{fso}), fines (V_{ffo}), rocks (V_{fro}) and balls (V_{fbo}). The flow-rates are defined as:

$$V_{fwo} = MIW, \tag{1}$$

$$V_{fso} = \frac{MFS}{D_S}(1-\alpha_r) \tag{2}$$

$$V_{ffo} = \frac{MFS}{D_S}\alpha_f \tag{3}$$

$$V_{fro} = \frac{MFS}{D_S}\alpha_r \tag{4}$$

$$V_{fbo} = \frac{MFB}{D_B} \tag{5}$$

The parameters α_f and α_r define the fraction of fines and rock respectively of the feed-rate of ore to the mill (MFS). By dividing the feed-rate of ore to the mill (MFS) and the feed-rate of balls to the mill (MFB) by the density of ore (D_S) and balls (D_B) respectively, the correct units are obtained. The implicit assumption when dividing by the ore density (D_S) in eq. (4) is that the ore is non-porous.

Although the feed-rate of ore to the mill (MFS) can be controlled fairly well, the variations in feed size and feed hardness upset the equilibrium in a mill significantly and are two of the main impediments to maintaining a mill at the optimum operating level (Napier-Munn et al., 1999).

3.2. Mill module

The mill module is the most crucial part of the circuit. This is where the valuable elements are liberated from the ore. The model for the mill accounts for the effect of slurry rheology and the mill power draw on the breakage of the ore.

The population volume balance of the hold-up of water (X_{mw}), solids (X_{ms}), fines (X_{mf}), rocks (X_{mr}) and balls (X_{mb}) in the mill are defined in terms of the inflow and outflow of each state:

$$\frac{d}{dt}X_{mw} = V_{mwi} - V_{mwo} \tag{6}$$

$$\frac{d}{dt}X_{ms} = V_{msi} - V_{mso} + RC \tag{7}$$

$$\frac{d}{dt}X_{mf} = V_{mfi} - V_{mfo} + FP \tag{8}$$

$$\frac{d}{dt}X_{mr} = V_{mri} - RC \tag{9}$$

$$\frac{d}{dt}X_{mb} = V_{mbi} - BC \tag{10}$$

where RC refers to rock consumption, BC refers to ball consumption and FP refers to fines production. These three breakage functions are described in eqs. (17), (18) and (19) respectively. The mill inlet flow-rates for water (V_{mwi}), solids (V_{msi}), fines (V_{mfi}), rocks (V_{mri}) and balls (V_{mbi}) are described in the equation below in terms of the feeder outflow defined in eqs. (1)-(5) and the cyclone underflow defined in eqs. (37), (40) and (41):

$$[V_{mwi}, V_{msi}, V_{mfi}, V_{mri}, V_{mbi}]^T =$$

$$[V_{fwo} + V_{cwu}, V_{fso} + V_{csu}, V_{ffo} + V_{cfu}, V_{fro}, V_{fbo}]^T \tag{11}$$

The mill outlet flow-rates for water (V_{mwo}), solids (V_{mso}), fines (V_{mfo}), rocks (V_{mro}) and balls (V_{mbo}) are defined in eqs. (20)-(23).

3.2.1. Rheology factor

It has been shown that slurry rheology is one of the factors that affect grinding mill performance (Shi and Napier-Munn, 2002). The empirically defined rheology factor (φ) is an attempt to incorporate the effect of the fluidity and density of the slurry on the milling circuit's performance. Random close packing of hard spheres cannot exceed approximately 64% of solids by volume, whereas random loose packing gives approximately 55% of solids by volume (Song et al., 2008). This means that the slurry in the mill cannot contain less than approximately 36% water by volume. For the fully mixed mill the solids in the slurry are not necessarily spherical. Therefore, the non-flowing slurry is approximated to contain 40% water by volume, and the maximum fraction of solids by volume of slurry (ε_{sv}) is 0.6. The volume of water is given by X_{mw} and the total volume of the slurry is given by the sum of the volume of water and solids ($X_{mw}+X_{ms}$), which results in the relation $X_{ms}/X_{mw} = 1.5 = (1/\varepsilon_{sv}-1)^{-1}$ for a non-flowing slurry. If the slurry is purely water, then $X_{ms}/X_{mw} = 0$. The function to describe the rheology factor (φ) is chosen to go from 1 for 100% water, to approximately 0.55 when the volume of solids (X_{ms}) is equal to the volume of water (X_{mw}), and to 0 for non-flowing mud at around 40% water by volume. Equation (12) achieves these three criteria and is plotted in Fig. 2.

$$\varphi = \left\{ \max\left[0, 1 - \left(\left(\frac{1}{\varepsilon_{sv}}\right) - 1\right)\frac{X_{ms}}{X_{mw}}\right]\right\}^{0.5} \tag{12}$$

The rheology factor (φ) is similar in concept to viscosity. To relate it to viscosity by a model is not particularly productive. The first problem is that the slurry is not a Newtonian fluid, so its stress-strain relationship is not defined by only one viscosity parameter. Even if the viscosity is modelled perfectly, assumptions and complex modelling would be necessary of how various amounts of balls, rocks, coarse material and slurry move in a mill. The motion of the charge in the mill is in turn a function of flow-rates, viscosities, the shape of lifters, the shape of the discharge grate, etc. Instead of using an intermediate variable (viscosity) that creates more questions than answers, the easily calculated rheology factor in eq. (12) characterises the fluidity of slurry. This rheology factor (φ) of the slurry can be used as a tool to model the effect of slurry water content on for example power draw and abrasion rates that depend on the thickness of the slurry.

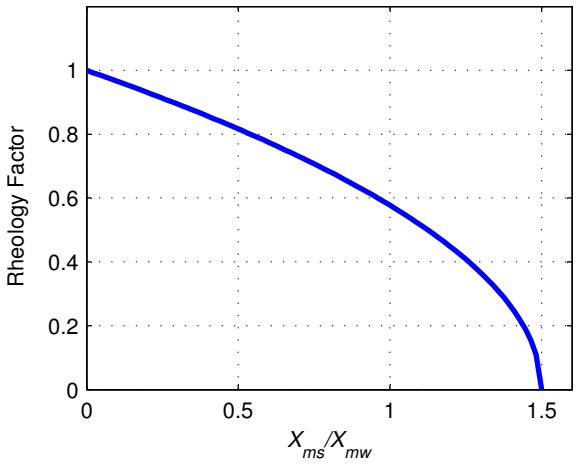

Figure 2: Rheology factor φ

3.2.2. Mill Power Draw

There are a number of mill power draw models that are valuable for the design and scale-up of grinding mills, such as the models found in Apelt et al. (2001), Austin (1990) and Morrell (2004). These models model mill power draw by means of a multi-parameter non-symmetrical curve as a function of the mass of material in the mill to make the power drop off suddenly as the mill becomes overfilled. However, the quick decline in mill power as the mill becomes overfilled is unlikely to only be due to the mass of the load. It is also due to a complicated effect of rheology that depends on water content and solids build-up within particular size classes. The complex interaction between water and solids concentrations and rheology and load cascading/sliding/tumbling still has to be solved comprehensively.

The mill power draw model presented here is made to rely on the lowest number of dependent variables that can be used to produce the required characteristics of the response. The power draw of the mill will be low for a very watery load and also for a load with low water content. In the first instance, the load forms a puddle at the bottom of the mill, whereas for low water content the load forms a ball of mud that rolls with little absorption of power. Somewhere in the middle the power reaches a maximum when the water content makes the load ride up the side of the mill to the maximum extent. Thus, the mill power draw can be modelled to depend on only two variables: the rheology factor of the slurry and the total charge inside the mill at which the maximum mill power draw occurs. For control purposes, accuracy far away from the maximum is not important, since the functional form of the mill power draw ensures that the power drops significantly and increasingly on both sides.

The mill power draw for the *Hulbert*-model is defined as:

$$P_{mill} = P_{max}\{1 - \delta_{Pv}Z_x^2 - 2\chi_P\delta_{Pv}\delta_{Ps}Z_xZ_r - \delta_{Ps}Z_r^2\} \cdot (\alpha_{speed})^{\alpha_P} \quad (13)$$

where P_{max} (kW) is the maximum mill motor power draw, δ_{Pv} and δ_{Ps} are the power-change parameters for volume and fraction solids respectively, χ_P is the cross-term for maximum power draw, α_{speed} is the fraction of critical mill speed and α_P is the fractional change in kW/fines produced per change in fractional filling of the mill. The effect of the total charge on mill power (Z_x) is given by the empirically defined equation:

$$Z_x = \frac{LOAD}{v_{mill} \cdot v_{P_{max}}} - 1 \quad (14)$$

where v_{mill} (m^3) is the volume of the mill, $v_{P_{max}}$ is the fraction of the mill filled for maximum power draw and $LOAD$ describes the mill charge volume in terms of the volumetric states in the mill:

$$LOAD = X_{mw} + X_{mr} + X_{ms} + X_{mb} \quad (15)$$

The effect of the slurry rheology on mill power (Z_r) is given by the empirically defined equation:

$$Z_r = \frac{\varphi}{\varphi_{P_{max}}} - 1 \quad (16)$$

where $\varphi_{P_{max}}$ is the rheology factor for maximum mill power draw. The significance of the parameters in eqs. (13)-(16) are discussed in consequent paragraphs.

As can be seen from eq. (13), the maximum mill power draw (P_{max}) is reached if the effect of slurry rheology (Z_r) and the effect of the charge in the mill (Z_x) on the mill power draw is zero, i.e. Z_r and Z_x are equal to zero. Two parameters are defined to achieve this: the rheology factor for maximum mill power draw $\varphi_{P_{max}}$ and the mill filling for maximum mill power draw $v_{P_{max}}$. Therefore, when $\frac{LOAD}{v_{mill}} = v_{P_{max}}$ and $\varphi = \varphi_{P_{max}}$, both Z_x and Z_r are zero.

The drop-off rate of the mill power draw (P_{mill}) is modelled as parabolic, with drop-off parameters for the effect of slurry rheology (Z_r) and the effect of the mill charge (Z_x) on the mill power draw. Thus, δ_{Ps} is the power-change parameter for the fraction of solids in the mill and δ_{Pv} is the power-change parameter for the total charge in the mill. The values for these two parameters depend on the dynamic response of the mill power draw of a plant to changes in the mill environment. By default they are set to unity, which results in a fast decrease/increase of the mill power draw to changes in the mill environment. If a slower response is needed, the values can be made lower. In general, sampling campaign data, good knowledge of the plant and simplifying assumptions are necessary to choose the parameter values with any accuracy.

The term $\chi_P\delta_{Pv}\delta_{Ps}Z_xZ_r$ in eq. (13) models the dependence of the maximum power draw with respect to one of

the variables (effect of rheology Z_r or effect of the charge Z_x) on the value of the other. The parameter χ_P determines the magnitude of this cross term for maximum power draw. It is unsure if this parameter should be positive or negative. If there is no mill power draw data available to support the fit of this parameter, the value for χ_P is chosen as zero.

Lastly, the mill power draw in eq. (13) is proportional to the speed at which the mill runs. The parameter introduced here is the fraction of the critical mill speed α_{speed}. This parameter is raised to the power α_P, the fractional power reduction per fractional reduction from critical mill speed. Unless survey data are available to fit this parameter, the value of α_P is chosen as unity.

In Powell et al. (2009, 2011) grindcurves are developed which relate mill filling to mill power draw. These studies give an indication of how a sampling campaign can be conducted to obtain the parameters mentioned above. An example of the effect that changes in the mill environment and the mill speed has on the power draw and the performance of an industrial grinding mill circuit can be seen in Viklund et al. (2006).

3.2.3. Breakage functions

As the ore grinds in the mill, it results in the consumption of rocks and balls over time, as well as the production of fines. The definition for rock consumption is:

$$RC = \frac{P_{mill} \cdot \varphi}{D_S \phi_r} \left(\frac{X_{mr}}{X_{mr} + X_{ms}} \right) \tag{17}$$

where ϕ_r (kWh/t) describes rock abrasion inside the mill, i.e. the rate at which rocks are consumed inside the mill. The mass of the ore hold-up inside the mill is given by $D_S \cdot (X_{mr} + X_{ms})$. The rheology factor ($\varphi$) is included in the rock consumption function in eq. (17) to model the effect of the density of the slurry on breakage. The abrasion rate of rocks is at its maximum in a watery grinding paste, represented by the rheology factor near 0.8. This is a practical finding - milling with more water gives a higher throughput with faster rock abrasion and a coarser grind. As the slurry becomes thicker, it cushions the interaction between the grinding media, and throughput drops, rock breakage rates decrease and the product becomes finer (Napier-Munn et al., 1999).

Ball consumption is defined as:

$$BC = \frac{P_{mill} \cdot \varphi}{\phi_b} \left(\frac{X_{mb}}{D_S \cdot (X_{mr} + X_{ms}) + D_B \cdot X_{mb}} \right) \tag{18}$$

where ϕ_b (kWh/t) is the steel abrasion factor, i.e. the rate at which balls are consumed within the mill. The mass of ore and balls in the mill is given by $D_S \cdot (X_{mr} + X_{ms}) + D_B \cdot X_{mb}$). The ball consumption equation follows the same reasoning as for rock consumption defined in eq. (17).

The production of fines in the mill is defined as:

$$FP = \frac{P_{mill}}{D_S \cdot \left\{ \phi_f \cdot \left[1 + \alpha_{\phi_f} \cdot \left(\frac{LOAD}{v_{mill}} - v_{P_{max}} \right) \right] \right\}} \tag{19}$$

where ϕ_f is the (kWh/t) is the power needed per tonne of fines produced and α_{ϕ_f} is the fractional change in power per fines produced per change in fractional filling of the mill. The fines produced from rocks are not distinguished from fines produced from the coarse ore. Therefore the fines production from rocks and coarse ore are lumped. If the mill operates at the optimal load volume for maximum mill power draw, eq. (19) reduces to $\frac{P_{mill}}{D_S \phi_f}$. The approximation of a rate of fines production per power input is considered an acceptable assumption for the reasons stated below. With more power, ore tends to break or wear away more even though only a small portion of the power goes into extra surface creation and most goes into heating. If one assumes breakage proportional to power, the error might be 5-15%. If one models breakage by the single particle breakage tests found in Napier-Munn et al. (1999), the results can be difficult to correct to 5-15% and the models do not necessarily relate power to breakage. The easily measurable power might be discarded even though it contains rich information about milling conditions. It is common to use the empirical connection between breakage rates and power, because it is easier to correlate with plant data and does not require extensive test work.

The rate of fines production per power input is not quite constant - it increases slightly when the mill filling is lower than the filling at which maximum power is drawn. For this reason the factor $\left[1 + \alpha_{\phi_f} \cdot \left(\frac{LOAD}{v_{mill}} - v_{P_{max}} \right) \right]$ is included in eq. (19), where α_{ϕ_f} accounts for the fractional change in power per fines produced per change in fractional filling of the mill. In other words, it is the slope of the power needed for a tonne of fines produced per volume of the mill filled. Unless survey data are available to determine the slope of the curve, a conservative value of α_{ϕ_f} is chosen as 0.01.

The rheology factor (φ) influences the breakage rate of fines indirectly by changing the modelled power draw (P_{mill}), which is assumed to be proportional to the breakage rate of fines. The power draw is a good intermediate variable since a mill running at relatively high power draw is invariably running at relatively high fines production rates. At present, there are no data or rationale to assume that the conversion of power draw (which is a function of fluidity) to fines production improves with higher fluidity or lower fluidity. For this reason the rheology factor (φ) is not included in eq. (19).

3.2.4. Discharge flow-rates

The discharge flow-rates of water (V_{mwo}), solids (V_{mso}), fines (V_{mfo}), rocks (V_{mro}) and balls (V_{mbo}) through the end-discharge screen are defined as:

$$V_{mwo} = V_V \cdot \varphi \cdot X_{mw} \cdot \left(\frac{X_{mw}}{X_{ms} + X_{mw}} \right) \tag{20}$$

$$V_{mso} = V_V \cdot \varphi \cdot X_{mw} \cdot \left(\frac{X_{ms}}{X_{ms} + X_{mw}} \right) \tag{21}$$

$$V_{mfo} = V_V \cdot \varphi \cdot X_{mw} \cdot \left(\frac{X_{mf}}{X_{ms} + X_{mw}} \right) \quad (22)$$

$$V_{mro} = V_{mbo} = 0 \quad (23)$$

where V_V is the volumetric flow per "flowing volume" driving force. The driving force is the pressure applied to the slurry to discharge from the mill. The hold-up of water (X_{mw}) and solids (X_{ms}) contained in the mill are the two main contributors to the driving force. Since the rheology factor (φ) already considers the effect of the volume of solids (X_{ms}), only the volume of water (X_{mw}) is multiplied with parameter V_V. Still, it is possible to multiply the sum of the volume of water and solids ($X_{mw}+X_{ms}$) instead of only the volume of water (X_{mw}) with the driving force in eqs. (20)-(22) above. The rheology factor (φ) is included to model the case of flow of the slurry through the discharge grate. The last term in brackets in eq. (20)-(22) provides the fraction of the relevant state of the volume of material that can be discharged from the mill. The flow-rate for rocks and balls (V_{mro} and V_{mbo}) out of the mill is zero since it is assumed rocks and balls are too large to discharge from the mill through the screen.

3.3. Mixed-sump module

For this module the assumption is made that the constituents inside the sump are fully mixed. This assumption is only valid if the sump is operated at the correct level, i.e. if the sump level is too low, air-entrainment could ensue; if the sump level is too high, a pool of stagnant liquid could form. Also, this assumption will only affect the dynamic response and not the steady-state response of the sump (Hinde and King, 1978).

The only constituents or states found in this module are water, solids and fines. The population volume balance of the hold-up of water (X_{sw}), solids (X_{ss}) and fines (X_{sf}) in the sump are defined as:

$$\frac{d}{dt} X_{sw} = V_{swi} - V_{swo} + SFW \quad (24)$$

$$\frac{d}{dt} X_{ss} = V_{ssi} - V_{sso} \quad (25)$$

$$\frac{d}{dt} X_{sf} = V_{sfi} - V_{sfo} \quad (26)$$

where V_{swi}, V_{ssi} and V_{sfi} represent the flow-rate of water, solids and fines into the sump respectively, and V_{swo}, V_{sso} and V_{sfo} represent the flow-rate of water, solids and fines out of the sump respectively. Equation (24) includes the flow-rate of water added to the slurry in the sump (SFW) to manipulate the density of the slurry feed to the cyclone. This density has a significant impact on the performance of the cyclone. The cyclone feed density is defined as $CFD = \frac{X_{sw}+D_s \cdot X_{ss}}{X_{sw}+X_{ss}}$ where the numerator gives the mass and the denominator the volume of the material that can be discharged from the sump.

The sump inflow of water (V_{swi}), solids (V_{ssi}) and fines (V_{sfi}) can be described in terms of the mill outflow defined in eqs. (20)-(22):

$$[V_{swi}, V_{ssi}, V_{sfi}]^T = [V_{mwo}, V_{mso}, V_{mfo}]^T \quad (27)$$

The sump discharge flow-rates of water (V_{swo}), solids (V_{swo}) and fines (V_{sfo}) are defined as:

$$V_{swo} = CFF \cdot \left(\frac{X_{sw}}{SVOL} \right) \quad (28)$$

$$V_{sso} = CFF \cdot \left(\frac{X_{ss}}{SVOL} \right) \quad (29)$$

$$V_{sfo} = CFF \cdot \left(\frac{X_{sf}}{SVOL} \right) \quad (30)$$

where CFF is the cyclone feed flow-rate and $SVOL$ is the volume of slurry in the sump:

$$SVOL = X_{sw} + X_{ss} \quad (31)$$

The cyclone feed flow-rate (CFF) is equal to the sum of V_{swo} and V_{sso}. The flow-rates defined in eqs. (28)-(30) are determined by multiplying the cyclone feed flow-rate (CFF) with the fraction of the volume which a state occupies within the total volume of the slurry inside of the sump.

3.4. Hydrocyclone module

Although the hydrocyclone model was briefly presented in Coetzee et al. (2010), a detailed description of the model equations is presented here. Because the dynamics of the hydrocyclone is much faster than the rest of the circuit, the hydrocyclone is described by a set of algebraic equations.

In the Plitt equation the corrected classification-size (d_{50_c}) is proportional to $\frac{exp(6.3F_i)}{(CFF)^{0.45}}$, where F_i is the fraction of solids in the total inflow volume and CFF is the cyclone feed flow-rate (Nageswararao et al., 2004). Thus, the definition of F_i is:

$$F_i = \frac{V_{csi}}{CFF} \quad (32)$$

where V_{csi} is the volumetric flow-rate of solids into the cyclone.

If the classification-size (d_{50_c}) increases, less coarse ore in the inflow to the cyclone (V_{cci}) will report to the underflow of the cyclone (V_{ccu}). It should be remembered that solids are defined as the sum of coarse ore and fine ore. Because the flow of coarse ore to the underflow (V_{ccu}) will constrain the flow of water to the underflow (V_{cwu}) and fines to the underflow (V_{cfu}), the actual split of coarse ore in the inflow to the cyclone (V_{cci}) needs to be determined before the split of fines that enter the cyclone (V_{cfi}) can be determined. Thus, the flow-rate of coarse ore at the underflow (V_{ccu}) is considered to be a function of:

- cyclone coarse ore inflow V_{cci}, as the primary dependency,
- cyclone feed flow-rate CFF, which determines the main centrifugal driving force in terms of inlet velocity,
- fraction of solids in the total inflow volume F_i, which relates to the degree of constrained rather than free particle movement, and
- the fraction of fines in feed solids P_i, which relates to viscosity and also indicates how much nearly-fine material is in the coarse fraction.

Accurate modelling of the low-flow conditions is not considered in the derivation of the model for the coarse split. Therefore, a functional form is used that gives a split between coarse ore underflow and inflow of $V_{ccu} = AV_{cci}$ as the cyclone feed flow-rate (CFF) becomes very small. The constant A can be used to shape the higher-flow part of the function instead of making the low-flow part accurate. From the Plitt equation, an increase in cyclone feed flow-rate (CFF) results in a reduction of the classification-size (d_{50_c}). Therefore, as the cyclone feed flow-rate (CFF) increases, the flow of coarse ore at the underflow (V_{ccu}) should increase asymptotically to the flow of coarse ore into the cyclone (V_{cci}). Thus, the sensitivity of the coarse material split to the total cyclone feed flow-rate is given by:

$$\left(\frac{V_{ccu}}{V_{cci}}\right)_1 = 1 - C_1 \cdot \exp\left(-CFF/\varepsilon_c\right) \tag{33}$$

where parameter C_1 relates to the split at low-flows when the centrifugal force is relatively small and the cyclone acts like a pipe T-piece, and parameter ε_c (m^3/h) defines how quickly the flow of coarse material to the overflow drops towards zero exponentially as a result of increasing centrifugal forces when the feed flow increases to high values. As seen from experimentation in Hulbert (2005), a prudent value for C_1 is 0.6. Equation (33) is plotted in Fig. 3a with parameter values as determined in Section 4.

The upper limit of the packing fraction of solid particles is approximately 0.6. Thus, the upper limit of the fraction solids in the feed (F_i) is 60%. As can be seen from the Plitt equation, the amount of coarse ore in the inflow (V_{cci}) that passes to the underflow (V_{ccu}) will decrease when the fraction solids in the feed (F_i) increases. This places a constraint on the coarse ore in the underflow (V_{ccu}) in terms of the fraction solids in the feed (F_i). Therefore:

$$\left(\frac{V_{ccu}}{V_{cci}}\right)_2 = 1 - \left(F_i/C_2\right)^{C_3} \tag{34}$$

where C_2 is a constant which normalises the fraction solids in the feed (F_i) according to the upper limit for the packing fraction of solid particles and C_3 determines the sharpness of the curve. Equation (34) is plotted in Fig. 3b with parameter values as determined in Section 4. This equation is unity when the fraction solids in the feed (F_i) is low. As the fraction solids in the feed (F_i) approaches that of thick mud (between 0.6 and 0.7), the relative movement of coarse material decreases towards zero. When this happens, the underflow is blocked and all the slurry goes to the overflow. Parameter C_3 defines the rate at which the equation above plunges towards zero. If C_3 is unity, the equation would be linear and not appropriate.

The last variable to consider for the coarse split model is the fraction fines in the feed solids (P_i). In terms of the inflow of fines (V_{cfi}) and solids (V_{csi}), P_i is defined as:

$$P_i = \frac{V_{cfi}}{V_{csi}} \tag{35}$$

If the fraction fines in the feed solids (P_i) is small, it indicates that the material is very coarse. Alternatively, if P_i is very large, it indicates the presence of more finer material in the coarse fraction. Therefore:

$$\left(\frac{V_{ccu}}{V_{cci}}\right)_3 = 1 - P_i^{C_4} \tag{36}$$

where C_4 is a constant which defines how quickly the function decreases towards zero. Equation (36) is plotted in Fig. 3c with parameter and flow-rate values as determined in Section 4. If the fraction of fines in the feed solids (P_i) is small, it indicates that the coarse material is very coarse. Alternatively, if the fraction of fines in the feed solids (P_i) is large, it indicates that there is more near-sized finer material in the coarse fraction. The effect starts at unity for low fines and decreases towards zero when almost all the solids in the feed material (V_{csi}) is fine. In this case, the small amount of coarse material is close to being fine and the viscous effects of a large volume of fines would hinder the settling movement of the coarse material.

The final underflow from the hydrocyclone to the mill for the coarse solids is defined as the multiplicative effect of the sensitivity of the coarse split to the total cyclone feed flow-rate (eq. (33)), of the sensitivity of the coarse split to the volume fraction of solids in the cyclone feed flow-rate (eq. (34)) and of the sensitivity of the coarse split to the fraction of fines in the solids feed flow-rate (eq. (36)):

$$\begin{aligned}\frac{V_{ccu}}{V_{cci}} &= \left(\frac{V_{ccu}}{V_{cci}}\right)_1 \left(\frac{V_{ccu}}{V_{cci}}\right)_2 \left(\frac{V_{ccu}}{V_{cci}}\right)_3 \\ &= \left(1 - C_1 e^{\left(\frac{-CFF}{\varepsilon_c}\right)}\right)\left(1 - \left(\frac{F_i}{C_2}\right)^{C_3}\right)\left(1 - P_i^{C_4}\right)\end{aligned} \tag{37}$$

To determine the amount of water and fines that accompany the coarse material to the underflow, the fraction of solids in the underflow volume (F_u) must be determined. This is modelled as a function of the fraction of solids in the inflow (F_i) as the primary dependency at low values of the coarse ore underflow (V_{ccu}), and the coarse ore underflow (V_{ccu}) as the primary dependency at high values of the coarse ore underflow (V_{ccu}). If V_{ccu} increases, it

is only logical that the fraction of solids in the underflow volume (F_u) should also increase. Again, the maximum packing fraction is approximated as 0.6, which places an upper limit on F_u. Therefore:

$$F_u = 0.6 - (0.6 - F_i) \cdot e^{(-V_{ccu}/(\alpha_{su}\varepsilon_c))} \tag{38}$$

where α_{su} relates to the fraction of solids in the underflow. Equation (38) is shown in Fig. 3d with parameter values as determined in Section 4. At around zero coarse ore underflow (V_{ccu}), the underflow consists primarily of feed material and $F_u \approx F_i$. As the flow of coarse material in underflow (V_{ccu}) increases, it increasingly squeezes the fines (V_{cfu}) and water (V_{cwu}) out of the underflow, asymptotically reaching the thickest possible mud at a solids fraction of about 0.6.

The fraction of solids in the underflow can also be written in terms of the underflow of fines (V_{cfu}), coarse ore (V_{ccu}) and water (V_{cwu}):

$$F_u = \frac{V_{cfu} + V_{ccu}}{V_{cwu} + V_{cfu} + V_{ccu}} \tag{39}$$

The ratio of fines to water in the overflow, underflow and cyclone feed is assumed to be the same, as the fines are considered to be fine enough not to be influenced by the centrifugal forces. Thus: $V_{cwu}/V_{cwi} = V_{cfu}/V_{cfi}$. With these ratios and eq. (39), the underflow of water (V_{cwu}) and fines (V_{cfu}) can be determined:

$$V_{cwu} = \frac{V_{cwi}\,(V_{ccu} - F_u V_{ccu})}{(F_u V_{cwi} + F_u V_{cfi} - V_{cfi})} \tag{40}$$

$$V_{cfu} = \frac{V_{cfi}\,(V_{ccu} - F_u V_{ccu})}{(F_u V_{cwi} + F_u V_{cfi} - V_{cfi})} \tag{41}$$

The cyclone inflow for water (V_{cwi}), coarse ore (V_{cci}), solids (V_{csi}) and fines (V_{cfi}) can be described in terms of the sump outflows defined in eqs. (28)-(30), as shown below.

$$[V_{cwi}, V_{cci}, V_{csi}, V_{cfi}]^T = [V_{swo}, V_{sso} - V_{sfo}, V_{sso}, V_{sfo}]^T \tag{42}$$

The product particle size (PSE) at the cyclone overflow is defined as the fraction of fines present in the total output flow of the cyclone:

$$PSE = \frac{V_{cfo}}{V_{cco} + V_{cfo}} = \frac{V_{cfi} - V_{cfu}}{V_{cci} - V_{ccu} + V_{cfo}} \tag{43}$$

where the V_{cfo} is the overflow of fines and V_{cco} is the overflow of coarse ore.

4. Parameter Estimation

4.1. Data for model fit

The data of five sampling campaigns on an existing single-stage grinding mill circuit at steady-state were provided by an industrial plant. The survey data gave the cumulative distribution of ore in 25 size classes for the inlet and outlet flows of each unit in the circuit. The key variables measured during the five surveys are shown in Table 4.

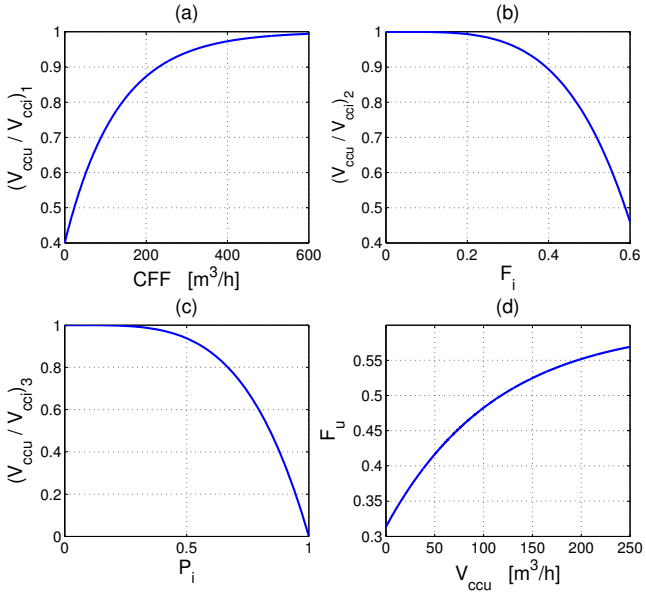

Figure 3: (a) Eq. (33): sensitivity of the coarse split to cyclone feed flow CFF. (b) Eq. (34): sensitivity of the coarse split to fraction solids in the cyclone feed flow F_i. (c) Eq. (36): sensitivity of the coarse split to fraction fines the feed solids P_i. (d) Eq. (38): sensitivity of fraction of solids in the underflow volume to the coarse ore underflow V_{ccu}.

Survey 3 presented the best results in terms of throughput, grind size, and energy efficiency. Therefore, the data from this survey are used to fit the parameters of the *Hulbert*-model. The other four surveys are used for the validation of the model.

During the sampling campaign, no attempt was made to estimate the ore, water and ball charge from crash stops and grind-out tests for each of the surveys. The only information received from the plant was that the mill was operated with a total charge filling of about 34% of mill volume. Therefore, the estimation for the total charge within the mill ($LOAD$) in eq. (15) is 20.1 m^3 for the third survey, given that the total mill volume (v_{mill}) is 59.12 m^3.

To determine the volume of slurry in the sump ($SVOL$) in eq. (31), it is known that the cross section of the sump is 1.1 m by 3.2 m, the height to the centre line of the pump is 0.7 m and the controlled slurry level above the pump inlet is 1.0 m. Therefore, $SVOL$ is estimated as 5.99 m^3.

It was stated by the plant that the mill was run at a constant ball charge of approximately 24% of the mill volume, which gives an estimate for the weight of the balls at $w_b = 66.8$ t. Also, the same type of ore is used for all the surveys. Thus, it is assumed that the total mass of balls within the mill and the size distribution of the ore feed remain constant for all five surveys.

Table 4: Survey data

Survey:	1	2	3	4	5
MIW (m^3/h)	4.71	4.45	4.64	3.66	4.22
MFS (t/h)	66.9	61.7	65.2	46.7	57.2
MFB (t/h)	6.43	5.38	5.69	6.77	6.58
SFW (m^3/h)	67.1	67.1	140.5	69.3	70.4
CFF (m^3/h)	267	224	374	294	305
PSE (Fraction)	0.60	0.55	0.67	0.68	0.58
P_{mill} (kW)	1142	1120	1183	1093	1071
Circ. Load Ratio	3.6	3.2	4.7	5.9	4.9
Specific Energy	17.1	18.2	18.1	23.4	18.7
kWh/t -75μm (ϕ_f)	31.5	36.9	29.6	37.6	35.7
Constants					
Ore Density (t/m^3)	3.2	Mill volume (m^3)			59.12
Ball Density (t/m^3)	7.85	Crit. mill speed			0.712

Table 5: Estimated parameter values and initial states

Parm	Value	Units	Parm	Value	Units
Mill and Feeder Parameters					
α_f	0.055	-	ϕ_b	90.0	kWh/t
α_r	0.465	-	ϕ_f	29.6	kWh/t
α_P	1	-	ϕ_r	6.03	kWh/t
α_{speed}	0.712	-	$\varphi_{P_{max}}$	0.57	-
α_{ϕ_f}	0.01	-	P_{max}	1662	kW
δ_{P_s}	0.5	-	v_{mill}	59.12	m^3
δ_{P_v}	0.5	-	$v_{P_{max}}$	0.34	-
D_B	7.85	t/m^3	V_V	84.0	-
D_S	3.2	t/m^3	χ_P	0	-
ε_{sv}	0.6	-			
Cyclone Parameters					
α_{su}	0.87	-	C_3	4	-
C_1	0.6	-	C_4	4	-
C_2	0.7	-	ε_c	129	m^3/h
States					
X_{mb}	8.51	m^3	X_{mw}	4.85	m^3
X_{mf}	1.09	m^3	X_{sf}	0.42	m^3
X_{mr}	1.82	m^3	X_{ss}	1.88	m^3
X_{ms}	4.90	m^3	X_{sw}	4.11	m^3

The sampling campaigns provided only steady-state values. No dynamic data were available for parameter estimation.

4.2. Hulbert-model parameter estimation procedure

The final estimated parameter values for the plant using the data of survey 3 are shown in Table 5. The procedure to determine the parameters relevant to each module is discussed below.

Before the model fit can start, it is necessary to define the passing sizes that the states of the *Hulbert*-model represent. The states are described in Table 6 in terms of the ore sizes and constituent they represent. The state X_{mr} represents the volume of ore in the mill above the discharge grate passing size. For the plant used to fit the model, the discharge grate allowed ore smaller than 22.4 mm to pass to the sump. The states X_{ms} and X_{ss} represent the volume of ore below 22.4 mm in the mill and sump respectively, i.e. the volume of solids in the mill and sump. The product specification size was 75 μm, which means that the states X_{mf} and X_{sf} are the volume of ore passing 75 μm in the mill and sump respectively, i.e. the volume of fines in the mill and sump. The states X_{mw} and X_{sw} are the volume of water in the mill and sump respectively, and X_{mb} is the volume of balls in the mill.

Table 6: Description of the states within the mill and sump

Constituents	Mill States	Sump States
Ore > 22.4 mm	X_{mr}	
Ore $\leq$ 22.4 mm	X_{ms}	X_{ss}
Ore $\leq$ 75 μm	X_{mf}	X_{sf}
Water	X_{mw}	X_{sw}
Balls	X_{mb}	

Table 7: The flow-rates of Survey 3 (Percentages are the cumulative percentage of ore passing size x_i)

Passing Size x_i	Feeder New Feed	Mill Inlet	Mill Outlet
22.4 mm	53.5%	91.9%	100%
0.075 mm	5.51%	11.5%	22.2%
Total ore (t/h)	65.2	374.7	374.7
Water (m^3/h)	4.64	115.9	115.9
Passing Size x_i	**Sump Dilution**	**Cyclone UF**	**Cyclone OF**
22.4 mm	-	100%	100%
0.075 mm	-	12.8%	66.8%
Total ore (t/h)	-	309.5	65.2
Water (m^3/h)	140.5	111.3	145.1

The cumulative distribution of ore for survey 3 passing each of the 25 size classes is plotted in Fig. 4. From this figure, the cumulative percentages of ore passing 22.4 mm and 75 μm are listed in Table 7. The table also shows the flow-rates of the total ore and water at the inlet and outlet of each unit. The data in Table 7 is used to estimate the parameters in the *Hulbert*-model.

4.2.1. Feeder

The feeder module has only two parameters to fit, α_r and α_f, where α_r is the fraction of ore in the feed that is larger than the aperture size of the discharge grate of the mill and α_f is the fraction of ore in the feed that is smaller than the final product specification size. The values for these two parameters can be obtained from the second column in Table 7: $\alpha_r = 0.465$ and $\alpha_f = 0.055$.

4.2.2. Mill

The first step in fitting the mill module parameters is to define the mill power draw parameters in eq. (13). It is assumed that the cross-term for maximum power (χ_P)

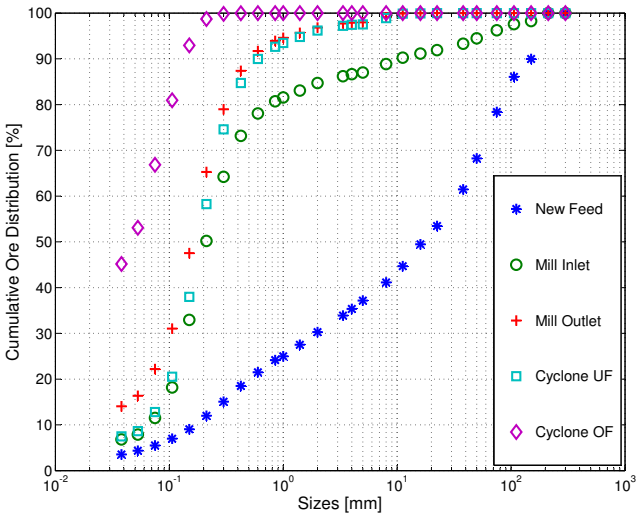

Figure 4: The cumulative ore distribution for survey 3 of the feeder outlet, the mill inlet and outlet, and the cyclone underflow (UF) and overflow (OF).

is zero and the fraction power reduction per fractional reduction from maximum mill speed (α_P) is unity since no data were available to fit these parameters. The plant provided time-series plots of the mill power draw, which gave an indication of the rate and magnitude of change in the mill power draw. From the plots provided by the plant, the power-change parameters for fraction solids (δ_{Ps}) and charge volume (δ_{Pv}) in the mill were set equal to 0.5.

Because the third survey provided the best results, and no additional information was available to determine the peak of the power-load curve, it is assumed that the data of the third survey represent the optimal operating condition of the grinding mill circuit. It is assumed that both the effect of the mill load (Z_x) and the effect of the slurry rheology (Z_r) on the mill power draw (P_{mill}) are zero and therefore $P_{mill} = P_{max}\left(\alpha_{speed}\right)^{\alpha_P}$. Given the critical mill speed (α_{speed}) and the mill power draw (P_{mill}) from survey data, it means that the maximum mill power draw is $P_{max} = 1183/0.712 = 1662$ kW.

If $Z_x = 0$, there is a constraint on the sum of the states in the mill:

$$X_{mw} + X_{mr} + X_{ms} + X_{mb} = v_{mill} v_{P_{max}} = LOAD \quad (44)$$

Because both the volume of the charge in the mill ($LOAD$) and the mill volume (v_{mill}) are known, it means that $v_{P_{max}} = 20.1/59.12 = 0.34$.

If $Z_r = 0$, the rheology factor for maximum mill power ($\varphi_{P_{max}}$) is equal to φ in eq. (12). It is not necessary to know the values of the volume of water (X_{mw}) and volume of solids (X_{ms}) in the mill to determine the rheology factor (φ), as only the ratio between the two is required. This ratio can be determined by dividing eq. (21) by (20):

$$\frac{V_{mso}}{V_{mwo}} = \frac{X_{ms}}{X_{mw}} \quad (45)$$

Thus, given that the maximum fraction of solids by volume of slurry (ε_{sv}) is fixed at 0.6:

$$\varphi_{P_{max}} = \left[1 - \left(\frac{1}{0.6} - 1\right)\frac{V_{mso}}{V_{mwo}}\right]^{0.5} = 0.572 \quad (46)$$

For the breakage functions, the abrasion rate of balls (ϕ_b) is specific to the type of steel used in the mill and is generally 90 kWh/t. The power needed per tonne of fines produced (ϕ_f) is provided by the survey data as 29.6 kWh/t. Because the ball mass (w_b) within the mill is known, the volume of balls in the mill is $X_{mb} = \frac{w_b}{D_B} = 8.51$ m^3.

There are six remaining unknown quantities within the mill: the abrasion rate of rocks (ϕ_r), the volumetric flow driving force (V_V) and the hold-up of water (X_{mw}), solids (X_{ms}), fines (X_{mf}) and rocks (X_{mr}) within the mill. The six equations used to calculate these unknowns are eqs. (9), (20), (21), (22), (44) and (45). Because the survey is conducted at steady state, the left-hand side of eq. (9) is equal to zero. The non-linear minimization function *fmincon* with the *Interior-Point* algorithm in the Optimisation Toolbox[1] of MATLAB was used to find the solution to the following equation:

$$\begin{aligned} 0 = & \left[V_{fro} - \frac{P_{mill}\varphi_{P_{max}}}{\phi_r D_S}\left(\frac{X_{mr}}{X_{mr}+X_{ms}}\right)\right]^2 \\ & + \left[V_{mwo} - \frac{V_V \varphi_{P_{max}} X_{mw}^2}{X_{mw}+X_{ms}}\right]^2 \\ & + \left[V_{mso} - \frac{V_V \varphi_{P_{max}} X_{mw} X_{ms}}{X_{mw}+X_{ms}}\right]^2 \\ & + \left[V_{mfo} - \frac{V_V \varphi_{P_{max}} X_{mw} X_{mf}}{X_{mw}+X_{ms}}\right]^2 \\ & + \left[LOAD - (X_{mw} + X_{ms} + X_{mr} + X_{mb})\right]^2 \\ & + \left[X_{ms} - \frac{X_{mw} V_{mso}}{V_{mwo}}\right]^2 \end{aligned} \quad (47)$$

The constraints for *fmincon* were chosen in light of the information provided by Table 7. Since the volume of the mill filled is $LOAD = 20.1$ m^3 and the volume of balls is $X_{mb} = 8.51$ m^3, there remains 11.6 m^3 to divide between the volume of solids (X_{ms}), rocks (X_{mr}) and water (X_{mw}) in the mill. Because the volumetric flow-rates of solids (V_{mso}) and water (V_{mwo}) out of the mill are almost equal according to Table 7, the volume of solids (X_{ms}) and water (X_{mw}) in the mill should be approximately equal according to eq. (45). Solids are the sum of fines and coarse ore, which means that the volume of fines (X_{mf}) should be less than the volume of solids (X_{ms}). According to Table 7, the volumetric flow-rate of rocks at the mill inlet (V_{mri}) is less than the volumetric flow-rate of solids at the mill inlet (V_{msi}). Thus, it is assumed that the volume of rocks (X_{mr}) in the mill is less than the volume of solids (X_{ms}). Insufficient survey data is available to choose narrow ranges for the volumetric flow driving force (V_V) and

[1] Optimisation Toolbox^{TM} is a registered trademark of The MathWorks, Inc.

the abrasion rate for rocks (ϕ_r). Therefore, the following constraints were chosen:

$$\begin{array}{l} 3 < X_{mw} < 6, \quad 3 < X_{ms} < 6, \quad 0 < X_{mr} < 3 \\ 0 < X_{mf} < 3, \quad 50 < V_V < 150, \quad 1 < \phi_r < 50 \end{array} \tag{48}$$

The result of the minimization of eq. (47) is $X_{mw} = 4.85$ m^3, $X_{ms} = 4.90$ m^3, $X_{mf} = 1.09$ m^3, $X_{mr} = 1.82$ m^3, $\phi_r = 6.03$ kWh/t and $V_V = 84.0$.

4.2.3. Sump

The three states within the sump can be determined from eq. (28)-(30) since the volume of slurry in the sump ($SVOL$), the cyclone feed flow-rate (CFF) and the flow-rates out of the sump (V_{swo}, V_{sso} and V_{sfo}) are all available from survey data. Thus:

$$X_{sw} = \frac{V_{swo} SVOL}{CFF} = 4.11 \text{ m}^3 \tag{49}$$

$$X_{ss} = \frac{V_{sso} SVOL}{CFF} = 1.88 \text{ m}^3 \tag{50}$$

$$X_{sf} = \frac{V_{sfo} SVOL}{CFF} = 0.42 \text{ m}^3 \tag{51}$$

4.2.4. Hydrocyclone

There are six parameters to determine for the hydrocyclone module (C_1, C_2, C_3, C_4, ε_c, α_{su}). These parameters are found in eqs. (37) and (38). Two equations and six unknowns leave four degrees of freedom. From the description of the hydrocyclone model in Section 3.4, C_1 is equal to 0.6 and C_2 is equal to 0.7. Hulbert (2005) indicated that equal integer values for C_3 and C_4 are practical. For the flow-rate data of the cyclone in Table 7, the smallest integer value that results in a positive value inside the natural logarithm in eq. (52) is $C_3 = C_4 = 4$. The calculation of the parameter related to coarse split (ε_c) and the parameter related to fraction solids in the underflow (α_{su}) is shown below:

$$\varepsilon_c = \frac{-V_{cti}}{\ln\left(\frac{1}{C_1} - \frac{V_{ccu}}{V_{cci} C_1 \left(1 - \left(\frac{F_i}{C_2}\right)^{C_3}\right)\left(1 - P_i^{C_4}\right)}\right)} = 129 \tag{52}$$

$$\alpha_{su} = \frac{-V_{ccu}}{\varepsilon_c \ln\left(\frac{F_u - 0.6}{F_i - 0.6}\right)} = 0.87 \tag{53}$$

5. Model Validation

A simulation platform was created in MATLAB and Simulink[2] to simulate the single-stage grinding mill circuit as described by the *Hulbert*-model. The platform was simulated for all five operating conditions of the sampling campaigns where the operating conditions are the five set-points for the grinding mill circuits.

In order to keep the sump from running dry or overflowing, a proportional-integral controller was used to keep the sump level at 1.0 m above the pump inlet by manipulating the cyclone feed flow-rate:

$$CFF = CFF_0 + K\left(e_l + \frac{1}{\tau}\int e_l dt\right) \tag{54}$$

where CFF_0 is the cyclone feed flow-rate of the third survey, $K = 20$ is the proportional gain, $\tau = 0.25$ is the integral reset and e_l is the error between the actual and desired sump level above the pump inlet.

5.1. Simulation

The manipulated variables in the simulation are the feed-rate of ore (MFS), water (MIW) and balls (MFB) to the mill, and the flow-rate of water to the sump (SFW), as described in Table 1. The simulation steps for these variables are shown in Fig. 5. The sequence of the input steps are as follows: Survey 3, Survey 4, Survey 5, Survey 1, Survey 2. The set of input variables that represent the operating condition of a survey are kept constant for 10 hours. Therefore, for the first 10 hours the model simulates the operating point of the third survey to which it was fitted. If a good fit was obtained, the output of the model should be similar to the actual steady-state outputs measured during the survey. When changing from one set-point to another, the input variables are ramped over a 10-hour period to reduce any excessive dynamic response in the output variables. The 10-hour period in which the manipulated variables are kept constant allows adequate time for the grinding mill to achieve a new steady-state and for any dynamic responses to have settled. It is in these 10-hour periods that the output variables of the simulation model can be compared with the actual steady-state sampling campaign data.

The *Hulbert*-model was simulated for two different cases. In the first, the power needed per tonne of fines produced (ϕ_f) was kept constant for all set-points at the value measured during the third survey. In the second case, the power needed per tonne of fines produced (ϕ_f) was updated at the start of each new set-point according to survey data shown in Table 4, i.e. ϕ_f is an additional input with set-point values as shown in Table 4.

5.2. Results and Discussion

The output variables that are of interest in the model validation procedure are the product particle size (PSE), the volume of slurry in the sump ($SVOL$), the cyclone feed flow (CFF), the mill power draw (P_{mill}) and the fraction of the mill filled. However, only PSE, CFF and P_{mill} can be compared to actual survey data. The other two variables were not measured during the surveys.

The simulation output of the volume of slurry in the sump ($SVOL$) and the fraction of mill filled are shown

[2]MATLAB and Simulink are registered trademarks of The MathWorks Inc.

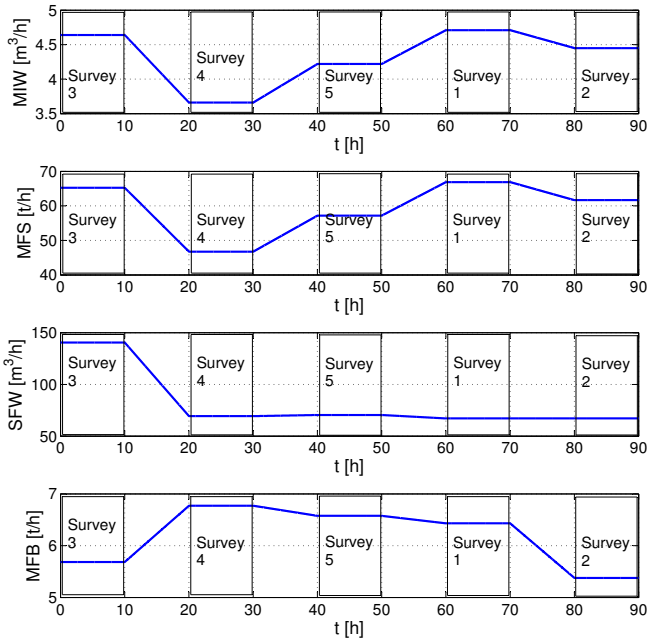

Figure 5: Inputs to grinding mill circuit

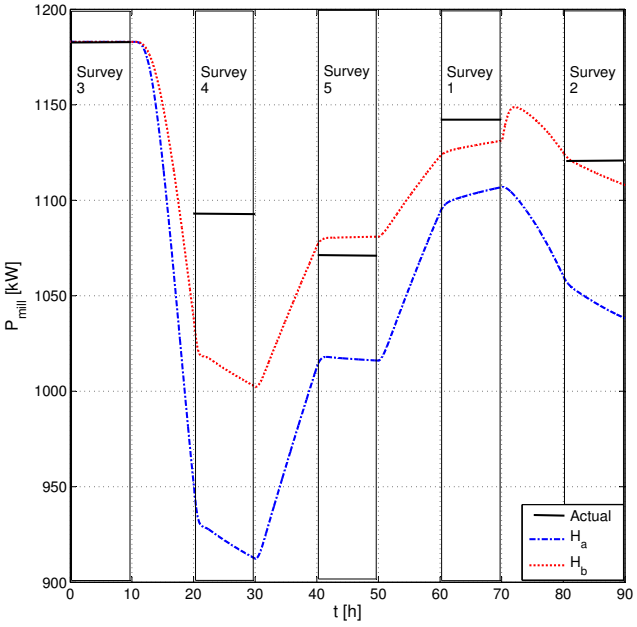

Figure 7: Mill power draw (P_{mill}). (Actual: sampling campaign data value, H_a: *Hulbert*-model with constant ϕ_f, H_b: *Hulbert*-model with updated ϕ_f)

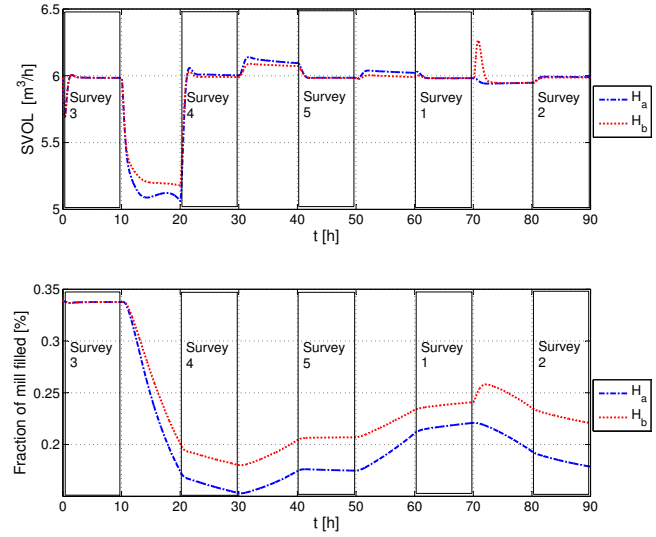

Figure 6: $SVOL$ and fraction of mill filled. (H_a: *Hulbert*-model with constant ϕ_f, H_b: *Hulbert*-model with updated ϕ_f)

in Fig. 6. The controller action is clearly visible in the $SVOL$. The significant change in $SVOL$ and fraction of milled filled between hours 10 and 20 is a result of the large reduction in the flow-rate of water to the sump (SFW) between surveys 3 and 4.

The mill power draw (P_{mill}) is shown in Fig. 7. The steady-state values measured during each survey are shown by the solid line. Figure 7 shows that the mill power draw was fitted accurately to survey 3, since P_{mill} given by eq. (13) and the measured mill power draw for the third survey are the same. The trend that P_{mill} follows over the period of the simulation is similar to the trend followed by the fraction of the mill filled in Fig. 6. The *Hulbert*-model seems to change in the right direction with and without the power needed per tonne of fines produced (ϕ_f) being updated. In the case where ϕ_f is updated, the model is able to give a fair estimate of the actual mill power for surveys 1, 2 and 5.

The cyclone feed flow-rate (CFF) is shown in Fig. 8. The steady-state values measured during each survey are shown by the solid lines. Figure 8 shows that CFF as given by the *Hulbert*-model was fitted accurately to survey 3, since CFF given by eq. (54) and the measured cyclone feed flow for the third survey are almost equal. However, the model could not accurately estimate CFF for the other surveys, apart from survey 2. Differences between the controller used by the actual plant and the controller used during simulation should not make a major difference on CFF in Fig. 8. At steady-state operation, the controller should no longer have any influence on CFF.

There are a few possible reasons for the poor estimation of CFF by the *Hulbert*-model for surveys 1, 4 and 5. The value of CFF is determined primarily by the flow-rate of water to the sump (SFW) plus how fast the mill discharges slurry. The latter is dependent on two factors in the mill: the viscosity (more water means higher flow) and the charge hold-up (higher volume means higher flow). These in turn are dependent on the flow-rate and content of water in the cyclone underflow (V_{cwu}). Because the cyclone underflow ties back to CFF, the main critical factor is the water content of the underflow. The higher CFF, the higher the water inflow, but the lower the water con-

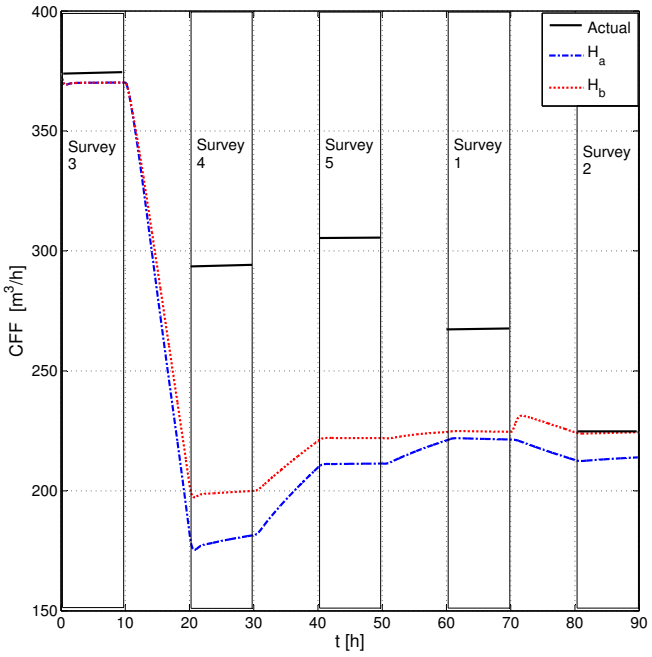

Figure 8: Cyclone Feed Flow. (Actual: sampling campaign data value, H_a: *Hulbert*-model with constant ϕ_f, H_b: *Hulbert*-model with updated ϕ_f)

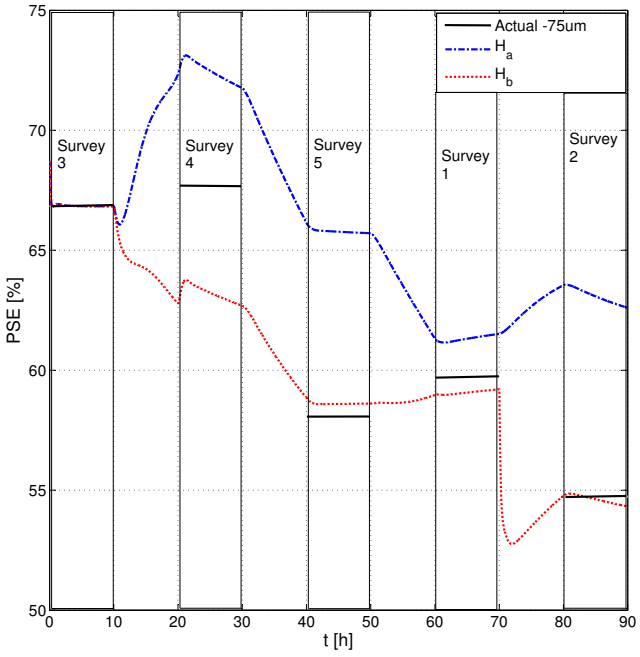

Figure 9: Particle Size Estimate. (Actual -75 μm: sampling campaign data value for ore passing 75 μm, H_a: *Hulbert*-model with constant ϕ_f, H_b: *Hulbert*-model with updated ϕ_f)

tent of the underflow. However, the ratio of fresh feed of solids and water to the mill can be higher or lower than the ratio of the recycle, which means the cumulative effect could be a positive or negative gain, or both in different regions.

The product particle size estimate (PSE) shown in Fig. 9 indicates the percentage of ore that passes 75 μm for each survey. The steady-state values measured during each survey are shown by the solid lines. This figure shows that the PSE as given by the *Hulbert*-model was fitted accurately to the data of the third survey. For the other surveys (except survey 4), the *Hulbert*-model gives a fair estimate of the actual percentage of ore that passes 75 μm when the power needed per tonne of fines produced (ϕ_f) is updated at the start of each new set-point. The accurate estimation of PSE for surveys 1, 2 and 5 when ϕ_f is updated is a good result since all the other model parameters remain fitted to the data of survey 3. In the case of a constant ϕ_f for all the surveys, the *Hulbert*-model struggles to follow the same trend as the measured PSE. Because the product particle size can be measured on-line in grinding mill circuits, it should be possible to calculate ϕ_f and update this parameter whenever the operating condition of the plant is altered.

The PSE should not be influenced extensively by the value of CFF. The cyclone splits off the coarse material back to the mill and makes the mill grind slightly differently. A high CFF tends to give particles a quicker interval between classification opportunities in the cyclone, reducing the fine material in the mill, making space for more coarse material to be ground and sharpening the slope of the size distribution of ore in the mill. The conditions in the mill are an integrated effect of the differences between inflows and outflows plus the effect of power and charge changes in the mill. The optimum fines production is determined by a sensitive balance of the conditions in the mill. Because grinding mill circuit operation normally chases the optimum condition, the gains of cause-and-effect are not large and linear near the optimum operating condition. Instead, the gains are relatively small and of either sign near the optimum. Therefore it is not surprising if PSE results at steady state are not predicted well when the power needed per tonne of fines produced (ϕ_f) is kept constant.

6. Conclusion

From Figs. 7-9 it is clear that the *Hulbert*-model was fitted satisfactorily to the data of the third survey. As the operating point is changed, the output variables of the model change in the correct directions with orders of magnitude similar to the changes in survey data. The *Hulbert*-model gives a qualitatively accurate description of the mill power draw (P_{mill}) for a constant and an updated power needed per tonne of fines produced (ϕ_f) and for product particle size estimate (PSE) for an updated power needed per tonne of fines produced (ϕ_f).

A general procedure to fit the *Hulbert*-model to any plant was described. The aim of the *Hulbert*-model is not to provide a tool for designing new grinding mill circuits. Rather, the model can be fitted to survey data with relative ease to provide a model that can be used to develop a

control strategy for a grinding mill circuit. If one assumes full-state feedback, the model can be used in a control strategy such as the robust non-linear model predictive controller in Coetzee et al. (2010). Otherwise, the model can be used as a state-estimator if the input and output variables of the plant are available.

The *Hulbert*-model was successfully fitted to actual plant data. The model was simulated and the results compared to the plant data. The model shows promise in estimating important process variables such as mill power and product particle size and is deemed suitable for process control studies.

This study is part of an ongoing endeavour to show the abilities of the *Hulbert*-model to be used as a tool for generating a good process model at low cost, developing a practical high-fidelity observer and designing an effective control strategy for a grinding mill circuit.

References

Amestica, R., Gonzalez, G. D., Menacho, J., Barria, J., March 1996. A mechanistic state equation model for semiautogenous mills. Int. J. Mineral Process. 44-45 (SPEC. ISS.), 349 – 360.

Apelt, T. A., Asprey, S. P., Thornhill, N. F., Feb. 2001. Inferential measurement of SAG mill parameters. Minerals Eng. 14 (6), 575–591.

Austin, L. G., 1990. A mill power equation for SAG mills. Minerals Metallurgical Process. 7 (1), 57–63.

Bauer, M., Craig, I. K., Jan. 2008. Economic assessment of advanced process control - A survey and framework. J. Process Control 18 (1), 2–18.

Coetzee, L. C., Craig, I. K., Kerrigan, E. C., Jan. 2010. Robust nonlinear model predictive control of a run-of-mine ore milling circuit. IEEE Trans. Control Syst. Technol. 18 (1), 222–229.

Craig, I., MacLeod, I., Jan. 1996. Robust controller design and implementation for a run-of-mine ore milling circuit. Control Eng. Practice 4 (1), 1–12.

Hinde, A. L., Kalala, J. T., April 2009. The application of a simplified approach to modelling tumbling mills, stirred media mills and HPGR's. Minerals Eng. 22 (7-8), 633–641.

Hinde, A. L., King, R. P., May 1978. Difficulties in the practical implementation of mill control systems. In: Proceedings of Eleventh Commonwealth Mining and Metallurgical Congress, Hong Kong.

Hulbert, D. G., 2005. Simulation of milling circuits: Part 1 & 2. Tech. rep., Mintek, Johannesburg, South Africa.

Hulbert, D. G., Craig, I. K., Coetzee, M. L., Tudor, D., 1990. Multivariable control of a run-of-mine milling circuit. J. South African Inst. Mining and Metallurgy 90 (7), 173–181.

Morrell, S., March 2004. A new autogenous and semi-autogenous mill model for scale-up, design and optimisation. Minerals Eng. 17 (3), 437–445.

Nageswararao, K., Wiseman, D. M., Napier-Munn, T. J., May 2004. Two empirical hydrocyclone models revisited. Minerals Eng. 17 (5), 671–687.

Napier-Munn, T. J., Morrell, S., Morrison, R. D., Kojovic, T., 1999. Mineral communition circuits: Their operation and optimisation, 2nd Edition. JKMRC Monograph Series in Mining and Mineral Processing.

Powell, M., Perkins, T., Mainza, A., 2011. Grindcurves applied to a range of SAG and AG mills. In: Proceedings of SAG 2011, Vancouver, B.C., Canada.

Powell, M., van der Westhuizen, A., Mainza, A., June 2009. Applying grindcurves to mill operation and optimisation. Minerals Eng. 22 (7-8), 625–632.

Shi, F. N., Napier-Munn, T. J., July 2002. Effects of slurry rheology on industrial grinding performance. Int. J. Mineral Process. 65 (3-4), 125–140.

Song, C., Wang, P., Makse, H. A., May 2008. A phase diagram for jammed matter. Nature 453 (7195), 629–632.

Stanley, G. G., 1987. The extractive metallurgy of gold in South Africa. Vol. 1. South African Institute of Mining and Metallurgy, Johannesburg.

Viklund, T., Albertsson, J., Burstedt, J., Isaksson, M., Soderlund, J., 2006. Evolution of AG mill control system at Boliden Mineral AB. In: Proceedings of SAG 2006, Vancouver, B.C., Canada.

Wei, D., Craig, I. K., Aug. 2009a. Economic performance assessment of two ROM ore milling circuit controllers. Minerals Eng. 22 (9-10), 826–839.

Wei, D., Craig, I. K., Feb. 2009b. Grinding mill circuits - A survey of control and economic concerns. Int. J. Mineral Process. 90 (1-4), 56 – 66.